MAUSAM, **77**, 2 (April 2026),199-210

MAUSAM

DOI: https://doi.org/10.54302/mausam.v77i2.7143
Homepage: https://mausamjournal.imd.gov.in/index.php/MAUSAM

UDC No.551.32(540.11)

Reconstruction of Paleo-glacier equilibrium line altitudes during the last glacial maximum in the Nubra-Shyok valley, Ladakh

PRANSHU BHARDWAJ*[1,2,3], Y.C. NAGAR[1], TEJPAL SINGH[2,3], M.S. SHEKHAR[1]

[1]*Defence Geoinformatics Research Establishment (DGRE), DRDO, Chandigarh-160036, India*

[2]*Academy of Scientific and Innovative Research (AcSIR), Ghaziabad- 201002, India*

[3]*CSIR- Central Scientific Instruments Organisation, Chandigarh- 160030, India*

(*Received 3 June 2025, Accepted 1 December 2025*)

***Corresponding author's email: pranshuofficial03@gmail.com**

सार – पश्चिमी हवाओं के प्रभुत्व वाले काराकोरम में पुरापाषाणकालीन जलवायु परिस्थितियों का पुनर्निर्माण, वैश्विक जलवायु परिवर्तनशीलता के प्रति उच्च-ऊंचाई वाले शुष्क क्षेत्रों की प्रतिक्रिया को समझने के लिए आवश्यक है। यह अध्ययन पूर्वी काराकोरम की नुब्रा-श्योक घाटी में स्थित 15 हिमनदों के लास्ट ग्लेशियल मैक्सिमम (एलजीएम) विस्तार का पुनर्निर्माण प्रस्तुत करता है, जिसमें संरक्षित हिमनदीय भू-आकृति विज्ञान का उपयोग ग्लारे मॉडल के संयोजन से किया गया है। मध्य-अक्षांश पश्चिमी हवाओं के प्रभाव क्षेत्र में स्थित यह घाटी, पश्चिमी हवाओं द्वारा संचालित हिमनदीय व्यवहार का आकलन करने के लिए एक असाधारण परिस्थिति प्रदान करती है। पुनर्निर्माण से पता चलता है कि मुख्य सियाचिन ट्रंक हिमनद (एनएस1) लगभग 692 वर्ग किमी क्षेत्र में फैला हुआ था, जिसमें मॉडल की गई बर्फ की मोटाई 200 से 400 मीटर के बीच थी, जो अधिकतम लगभग 370 मीटर तक पहुँचती थी। संतुलन रेखा ऊँचाई (ईएलए) का अनुमान चार स्थापित भू-आकृति विज्ञान पद्धतियों (एएबीआर, एएआर, एमईएलएम और टीएचएआर) के भारित माध्य का उपयोग करके लगाया गया था। परिणामों से पता चलता है कि एलजीएम के दौरान सियाचिन ग्लेशियर के लिए ईएलए में लगभग 700 मीटर की उल्लेखनीय गिरावट आई थी। स्थानीय रूप से प्राप्त लैप्स दर के आधार पर, यह ईएलए गिरावट गर्मियों के तापमान में 1.5-2.0 डिग्री सेल्सियस की कमी के अनुरूप है, जिससे पता चलता है कि पश्चिमी हवाओं से प्रेरित वर्षण ने वैश्विक एलजीएम शीतलन के क्षेत्रीय प्रभाव को कम किया। एक विशिष्ट स्थानिक ईएलए पैटर्न भी स्पष्ट है: पूर्व की ओर मुख वाले ग्लेशियर पश्चिम की ओर मुख वाले ग्लेशियरों की तुलना में काफी अधिक मान दर्शाते हैं। यह विषमता पश्चिमी हवाओं द्वारा नियंत्रित नमी वितरण और अपक्षरण प्रक्रियाओं को प्रभावित करने वाले विभेदक सौर ताप के संयुक्त प्रभावों को दर्शाती है। ये निष्कर्ष घाटी में एलजीएम हिमनदीकरण की सीमा और प्रचलित पुरापाषाण जलवायु परिस्थितियों पर ठोस मात्रात्मक सीमाएं प्रदान करते हैं, जो हिमालय के इस उच्च-ऊंचाई वाले क्षेत्र में ग्लेशियर गतिशीलता और तापमान व्यवस्था को नियंत्रित करने में मध्य-अक्षांश पश्चिमी हवाओं के प्राथमिक प्रभाव को उजागर करते हैं।

ABSTRACT. Reconstructing paleoclimatic conditions in the westerlies-dominated Karakoram is essential for understanding the response of high-altitude arid regions to global climate variability. This study presents a reconstruction of the Last Glacial Maximum (LGM) extents of 15 glaciers in the Nubra–Shyok valley, eastern Karakoram, using preserved glacial geomorphology in combination with the GlaRe model. The valley, situated within the influence zone of the mid-latitude Westerlies, provides an exceptional setting to assess westerlies-driven glacial behavior. The reconstructions indicate that the main Siachen trunk glacier (NS1) covered an area of approximately 692 km², with modeled ice thicknesses ranging between 200 and 400 m, reaching a maximum of about 370 m. Equilibrium Line Altitudes (ELAs) were estimated using a weighted average of four established geomorphometric approaches (AABR, AAR, MELM, and THAR). The results indicate a marked ELA depression of ~ 700 m for the Siachen glacier during the LGM. Based on a locally derived lapse rate, this ELA depression corresponds to the lowering of summer temperature by 1.5–2.0 °C, suggesting that enhanced westerlies-induced precipitation moderated the regional expression of global LGM cooling. A distinct spatial ELA pattern is also evident: east-facing glaciers show significantly higher values than west-facing glaciers. This asymmetry reflects the combined effects of westerlies-controlled moisture distribution and differential solar insolation influencing ablation processes. These findings provide robust quantitative constraints on the

extent of LGM glaciation and the prevailing paleoclimatic conditions in the valley, highlighting the primary influence of mid-latitude westerlies in modulating glacier dynamics and temperature regimes across this high-elevation region of the Himalaya.

Key words – Himalayas, Nubra-Shyok valley, ELA, AABR, Glacier reconstruction, Hypsometry.

1. Introduction

The mountain glaciers and ice caps are among the most sensitive components of the cryosphere and serve as critical indicators of climate variability (Oerlemans, 2005; Haeberli *et al*., 2009). Within the High Mountain Asia region comprising the Himalaya, Karakoram and Hindu Kush ranges, these glaciers contain the largest volume of ice outside the polar regions. They constitute vital freshwater reserves that regulate the hydrological regimes of major river systems including the Indus, Ganges and Brahmaputra, sustaining hundreds of millions of people downstream (Immerzeel *et al*., 2010; Bolch *et al*., 2012). Understanding how these glaciers have responded to past climatic fluctuations is therefore crucial not only for reconstructing Quaternary paleoclimates but also for anticipating future water security under ongoing global warming.

The Karakoram Range, in particular, presents a climatologically distinct and complex sector of the HMA. In contrast to the monsoon-dominated Greater Himalaya, the Karakoram and the adjacent Trans-Himalayan valleys, including the Nubra-Shyok Valley, lie within a high-altitude arid zone predominantly influenced by mid-latitude westerlies (Dash *et al*., 2004; Palazzi *et al*., 2013). These contribute the vast majority of annual accumulation in the form of winter and early spring snowfall (Bhutiyani *et al*., 2010; Shekhar *et al*., 2017). As a result, many glaciers in this region exhibit anomalous behavior remaining stable or even advancing while widespread retreat dominates much of the Himalaya (Hewitt, 2005; Bolch *et al*., 2012). This paradox highlights a fundamental question; how did this westerlies-dominated cryosphere region respond during a period of global maximum cooling such as the Last Glacial Maximum (LGM; ~26.5–19 ka). One of the most crucial approaches to addressing this question is through the reconstruction of paleo–Equilibrium Line Altitudes (ELAs). The ELA, defined as the average elevation where annual accumulation equals annual ablation, represents a first-order proxy for glacier mass balance and is directly governed by local temperature and precipitation (Benn & Lehmkuhl, 2000; Porter, 2000; Cogley *et al*., 2010). Reconstructing paleo-ELA and comparing them to modern values provides a quantitative measure of ELA depression, thereby constraining the magnitude of past temperature and precipitation changes.

Previous investigations in the Karakoram & Ladakh region reveal a complex and often asynchronous glacial chronology (Owen & Benn, 2005; Owen & Dortch, 2014). Cosmogenic ^{10}Be surface exposure dating from the Nubra-Shyok confluence identified three major glacial stages: Deshkit 3 (~144 ka), Deshkit 2 (~81ka), & Deshkit 1 (~45 ka) with the youngest (Deshkit 1) corresponding to an ELA depression of ~ 290 m (Dortch *et al*., 2010). However, this chronology has been contradicted by subsequent studies using Optically Stimulated Luminescence (OSL) dating. The significantly younger ages, documenting major advances precisely within the LGM (MIS-2) at ~ 24 ka and ~18 ka were presented by Nagar *et al*. (2013) and Ganju *et al*. (2018). More recent, detailed chronologies (Sharma *et al*., 2018; Bhardwaj *et al*., 2024) have confirmed a highly dynamic Late Quaternary history, identifying distinct deposits from the LGM (~18.4 ka at Agham), the Late Glacial (~14.5 ka at Changmar), the Younger Dryas (~12-10 ka at Khardung), and multiple Holocene/Neoglacial advances (~0.4 ka at Chalunka). This finding of a significant LGM (MIS-2) glaciation aligns the region more closely with neighboring catchments, such as the Pir-Panjal, where MIS-2 ELA depression of ~350 to 670 m were reported (Paul *et al*., 2022), and the Markha–Nimaling valleys, which also show substantial LGM lowering (Damm, 2006). They highlight that variations in topography, debris cover, and local microclimates exert strong controls on glacier mass balance, complicating region-wide correlation.

Despite an evolving geochronological & climato-logical database, quantitative reconstructions of LGM glacier geometries and ELAs within the Nubra-Shyok valley remain scarce. In this study, we hypothesize that during the LGM, glaciers in the valley were primarily sustained by enhanced westerly-derived winter accumulation, resulting in glacier geometries and ELA depression more characteristic to those of the Karakoram rather than the monsoon-dominated Greater Himalaya (Benn & Owen, 1998; Murari *et al*., 2014). This interpretation is consistent with broader paleoclimate reconstructions indicating a southward shift intensification of the westerlies during the global LGM (Herzschuh, 2006). Accordingly, the aim of this study is to:

(i) Reconstruct LGM glacier geometry and ice thickness using the GlaRe model constrained by field and geomorphic evidence; (ii) Estimate paleo-ELA for fifteen

glaciers using a robust, weighted-average approach integrating four established methods (AABR, AAR, MELM and THAR);

(iii) Calculate the total ELA depression relative to present conditions; and

(iv) Analyze spatial trends in reconstructed ELAs to infer the climatic forcing particularly the dominance of westerlies versus monsoonal influence during the LGM.

2. Data and methodology

2.1 *The Study Area*

2.1.1 *Geological Setting*

The Nubra-Shyok Valley is wedged between the Karakoram Range to the north & the Ladakh Range to the south. The geology of the region is a complex assemblage resulting from the collision of the Indian and Eurasian plates. The north of the Ladakh Batholith is accompanied by a substantial succession of Khardung Volcanics, which are overthrust by the tectonic ophiolitic melange of the Shyok Formation. This formation is, in turn, intruded by the Karakoram Batholith (Thakur and Misra, 1984). The valley is structurally controlled by two major tectonic features: the Karakoram Fault (KF) and the Shyok Suture Zone (SSZ). The KF is a dominant, 700 km-long dextral (right-lateral) strike-slip fault that segregates the Ladakh and Karakoram terrains at their confluence (Upadhyay *et al*., 1999; Searle *et al*., 1998). Near the settlement of Tirith, at the confluence west of Khalsar, lies the Saltoro Block, which is composed of ophiolite, granitoids, and greenschist metamorphic rocks that have undergone profound deformation (Weinberg and Searle, 1998). This active tectonic setting is directly responsible for the region's extreme vertical relief and plays a significant role in controlling drainage patterns and landscape evolution.

2.1.2. *Climatic and geographic setting*

The Nubra-Shyok valley is a high-altitude, cold, and arid landscape, geographically situated in the rain-shadow of the Greater Himalayan range. This orographic barrier limits moisture from the ISM, creating a unique climatic regime dominated by the westerlies (Owen and Benn, 2005). The westerlies are the primary source of precipitation for the region, arriving during the winter (November–April) and depositing the majority of accumulation as snow. This seasonal snowpack is the principal driver of glacier mass balance in the Karakoram (Dash *et al*., 2004; Bhutiyani *et al*., 2010). The dominance of the westerlies is evident in the regional glacier distribution, as glacier length generally decreases from west to east while the Karakoram range effectively blocking the incoming moisture (Raina and Sangewar, 2007). The Siachen Glacier (~74 km), the second-longest glacier outside the poles and the source of the Nubra River, is direct evidence of this moisture-trapping.

While the ISM's influence is secondary, it contributes approximately one-third of the annual moisture, primarily during the summer months (Bhutiyani *et al*., 2010). The total annual precipitation in the valley, however, remains low, averaging approximately ~300 mm/year (Chevuturi *et al*., 2018). Furthermore, the broader Western Himalayan region, including this area, is subject to high-intensity, short-duration extreme precipitation events that have significant geomorphic impacts (Shekhar *et al*., 2017). This interplay between the westerlies and the ISM, combined with the active tectonic setting, governs the glacial, fluvial, and aeolian processes that have shaped the Quaternary landscape.

This study employs an integrated geomorphic and physics-based framework to reconstruct the LGM glacier extents and their corresponding ELAs. The approach follows established protocols used in Himalayan paleo-glaciology (Paul *et al*., 2022) and comprises four sequential stages: (1) data acquisition and geomorphic mapping; (2) paleo-glacier surface reconstruction using shear-stress; (3) paleo-ELA estimation; and (4) determination of present-day ELA and the magnitude of ELA depression.

2.2. *Data sources and geomorphic mapping*

The reconstruction of glacial extent and paleo-ELA for the valley of the study area was carried out using multi-source remote sensing datasets, including Google Earth imagery, Landsat TM, and ASTER (Advanced Spaceborne Thermal Emission and Reflection Radiometer) DEMs. A False Color Composite (FCC) of Landsat-8 imagery was draped over the DEM to enhance the visual identification of glacial geomorphic features, an approach widely recognized as effective for delineating moraines and other glacial landforms (Greenwood and Clark, 2009). The shaded-relief rendering of the DEM further helped 3D visualization, particularly in identifying moraine ridges and valley morphology (Jansson and Glasser, 2005; Greenwood and Clark, 2009). During field investigations, some characteristic glacial geomorphic features such as lateral and terminal moraines, and U-shaped valleys were identified and verified on-site, providing field-based support for the remotely mapped glacial extents. The distinct erosional and depositional landforms, including moraines, outwash plains, and arêtes, are well preserved within the region, offering clear geomorphic evidence for reconstructing glacier extents.

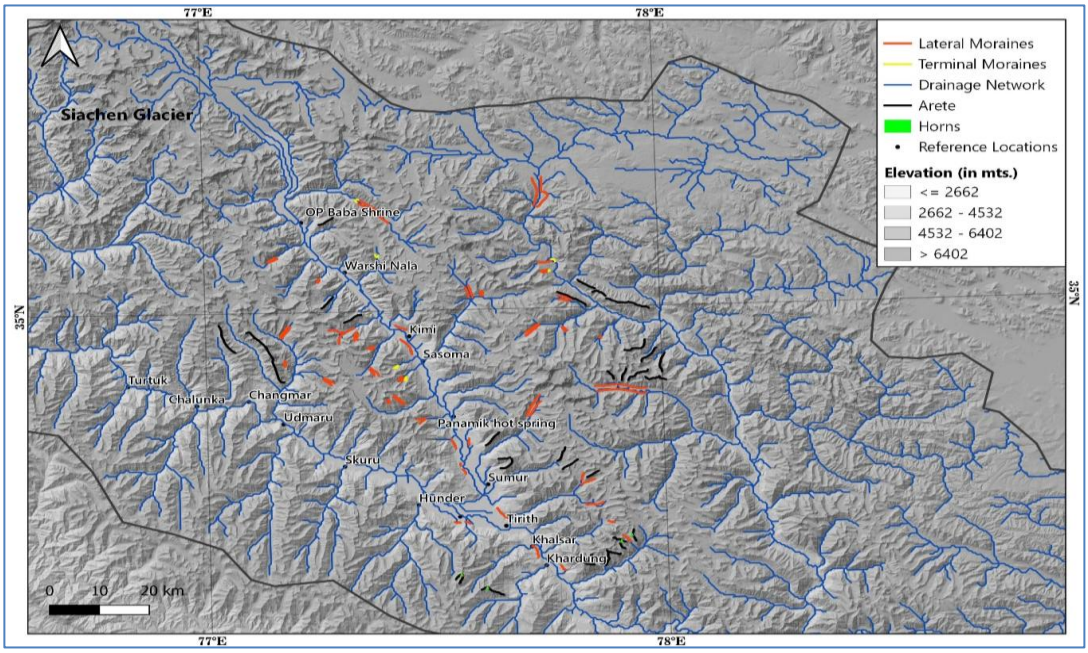

Fig. 1. The study area map showing Nubra-Shyok valley with DEM derived hillshade, marked locations, drainage network and geomorphic features specifically moraines, aretes and horns

2.3. *Paleo-glacier reconstruction*

The three-dimensional reconstructions of 15 paleo-glaciers were generated using the GlaRe model for ArcGIS (Pellitero *et al*., 2016). This tool employs a Python-based workflow to estimate ice thickness (h) from the perfect-plasticity basal shear stress relationship (Nye, 1952 a, b) given below

$$\tau_b = \rho g h \sin\alpha$$

where τ_b is the basal shear stress, ρ the density of ice (900 kg m^{-3}), g the gravitational acceleration (9.81 m s^{-2}), h the ice thickness (~390 m derived by measuring the elevation difference between the glacier valley bottom and its bounding valley shoulders), and α the surface slope (average: 25° to 28°).

For this reconstruction, a basal shear stress (τ_b) of 100 kPa (1 bar) was used. This value is a widely accepted standard for temperate valley glaciers. However, it was not applied as a uniform default. Instead, the shear stress was iteratively tuned for each glacier. The model was run, and the resulting ice surface elevation was compared to the digitized elevations of the constraining lateral moraine crests. The shear stress was adjusted until the modeled ice surface achieved the best possible fit with the physical moraine evidence, ensuring a robust and geomorphologically-validated reconstruction. The glacier flowlines, which serve as the basis for ice-thickness computation, were generated from the SRTM DEM (30 m resolution). For most glaciers, flowlines were manually digitized along the centerline of the deglaciated valleys following topographic gradients and valley morphology, while for others, they were automatically derived using GlaRe's flowline creation tool. The resulting ice-thickness and surface-elevation data were used to estimate the ELAs for each glacier.

2.4. *Paleo-ELA calculation*

The 15 reconstructed glacier surfaces, the paleo-ELA was calculated using four established methods. The Accumulation Area Ratio (AAR) method was applied assuming a standard steady-state ratio of 0.58 (Benn and Lehmkuhl, 2000). The Area-Altitude Balance Ratio (AABR) method, a more refined hypsometric approach, was also used, applying a balance ratio of 1.58 to solve for the altitude of zero net balance (Rea, 2009). For a geometric-based estimate, the Toe-to-Headwall Altitude Ratio (THAR) was calculated using a fixed ratio of 0.4 between the glacier's lowest (toe) and highest (headwall) points (Kurowski, 1891). Finally, the Maximum Elevation of Lateral Moraines (MELM), a field-based proxy that uses the highest preserved altitude of the lateral moraine crests, was also determined (Pellitero *et al*.,2015). Given the known variability, a Weighted Average (WA) was calculated to determine the most representative paleo-ELA, following established best practices (Benn and Lehmkuhl, 2000; Paul *et al*., 2022). This scheme assigns the highest confidence to the hypsometry-based AABR and AAR methods, which are considered the most glaciologically robust (Osmaston, 2005; Pellitero *et al*., 2015).

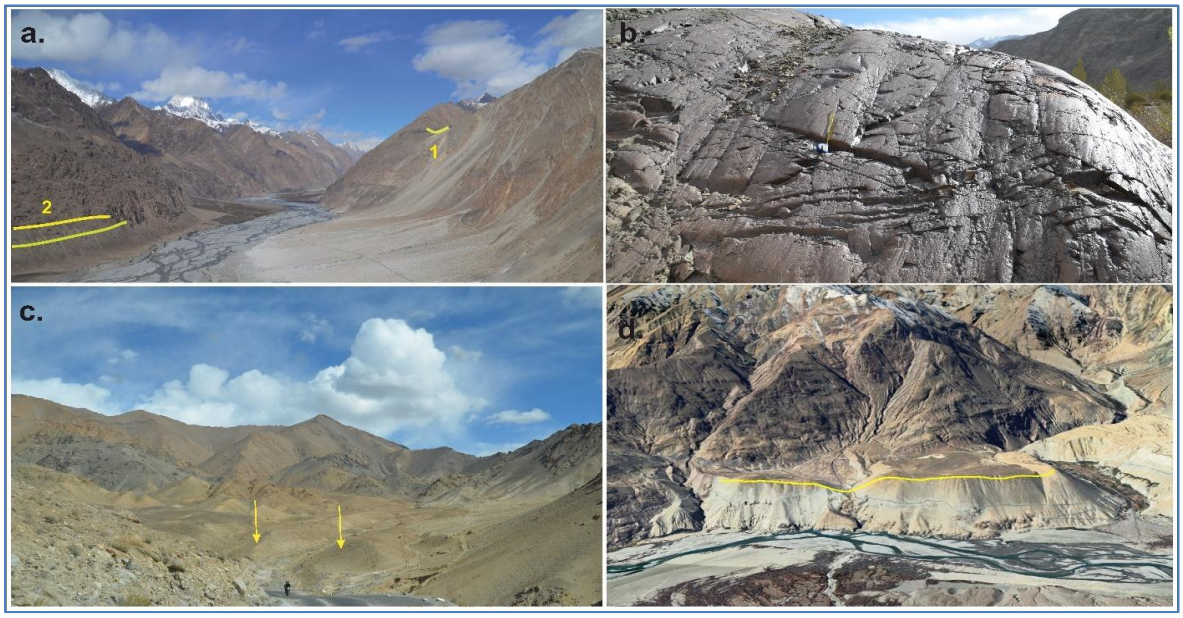

Fig. 2. Field photographs showing (a) Upstream view of the Nubra Valley from Sasoma showing prominent lateral moraines (2) along the right flank of the valley. A tributary valley (1) exhibits remnant terminal moraines hanging along its walls. (b) Striations observed on boulder surfaces indicate the direction of former ice movement. (c) Well-preserved lateral moraines are visible around Tirith and Diskit in the Nubra Valley. (d) Google Earth imagery showing the preserved moraine in Khalsar.

2.5. *Present-day ELA and ELA Depression*

To provide a baseline for comparison, the present-day ELA was calculated. The modern glacier outlines were acquired from the Global Land Ice Measurements from Space (GLIMS 2018) and Google Earth database. Using the SRTM DEM, the AABR method was applied to these glaciers to calculate the present-day ELA. The LGM ELA depression was then determined as the arithmetic difference between the calculated WA paleo-ELA and the modern AABR-derived ELA.

3. Results and discussion

3.1. *Glacial Landforms*

The Nubra-Shyok valley provides an exceptional record of Quaternary landscape change due to the preservation of geomorphic features. The regional landscape is a complex assemblage resulting from the interplay of glacial, fluvial, mass wasting, and periglacial processes (Juyal *et al*., 2014; Hakhoo *et al*., 2019). While the valley consists of glacial and associated landforms including extensive alluvial fans, U-shaped troughs, polished surfaces, striations, and thick fluvio-lacustrine deposits; the primary focus of this investigation is the depositional ridges that directly delimit former ice extents. As such, the lateral and terminal moraines are the most critical landforms for this study. These distinct, mappable ridges are supraglacial depositional structures that provide direct, physical evidence of the historical extent and area of the LGM paleo-glaciers.

Fig. 1. presents the detailed geomorphological map of the study area. The prominent and well-preserved moraines were identified between the Siachen glacier's snout and the Nubra-Shyok confluence, particularly near the settlement of Tirith. Additionally, distinct lateral moraines were mapped at the confluence of Khardung Nala and the lower Shyok valley. The erosional features, including sharp-crested arêtes and horns, were also systematically mapped. These mapped geomorphic features collectively provide the empirical constraints for the subsequent glacier reconstructions.

During field investigations, clear geomorphic evidence of past glaciation was observed, including lateral moraines, polished boulders exhibiting striations, and perched moraine ridges along the valley flanks (Fig. 2).

3.2. *Paleo-glacier reconstruction*

The 15 reconstructed paleo-glaciers (NS1-NS15) are visually presented in Fig. 3 as red lines. This includes the extensive Siachen trunk glacier (NS1) and the 14 tributary valley glaciers. The total reconstructed area for the 15 glaciers shows significant variation, ranging from 1.63 km² (NS10) to 691.63 km² (NS1). The hypsometry of the glaciers also serves as is an important quantification

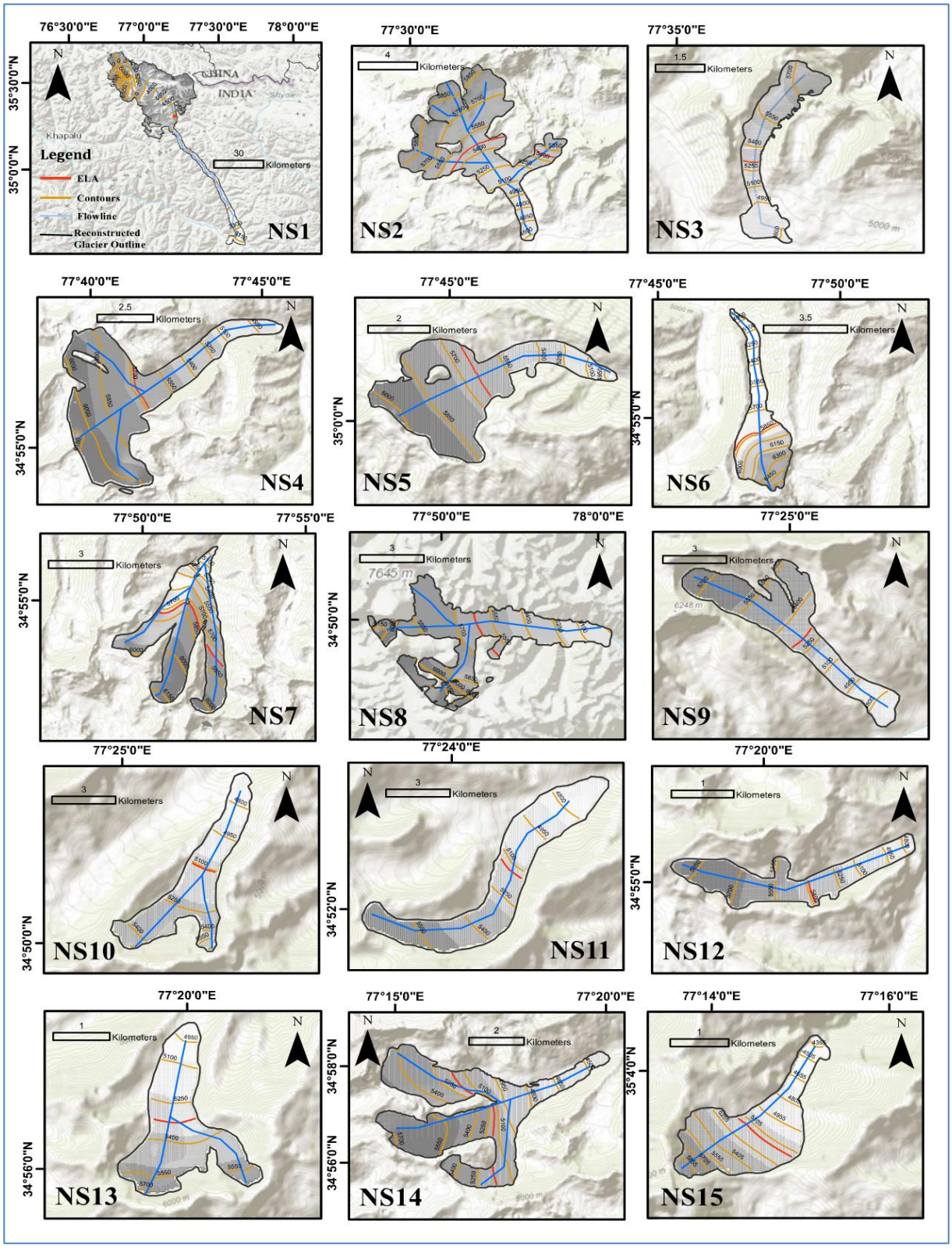

Fig. 3. Reconstructed LGM glacial extents of 15 glaciers of Nubra-Shyok valley. Note acronym NS stands for Nubra-Shyok valley from 1-15

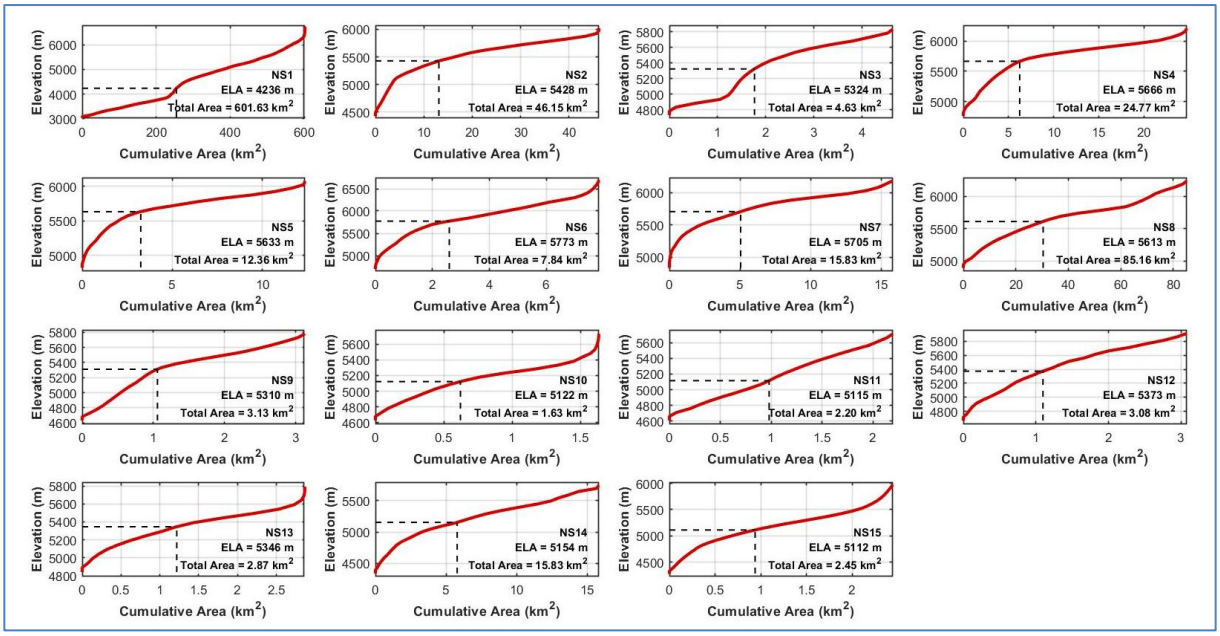

Fig. 4. Hypsometric curves for the 15 reconstructed glaciers in the Nubra-Shyok valley. Each plot (NS1–NS15) shows the area-elevation distribution, plotting elevation (m) against normalized cumulative area (km²). The final calculated weighted average paleo-ELA and the total reconstructed LGM area are marked for each glacier.

TABLE 1

Showing the paleo-ELA values estimated by using different ELA methods and then taking weighted average of all the methods to obtain a single value. The weight assigned to each method is mentioned in the table.

Weightage	50%	30%	5%	15%	100%
Glaciers/Methods	AABR	AAR	MELM	THAR	WA/ PaleoELA
NS 1	4317	4067	3549	4536	4236
NS 2	5499	5599	4753	5076	5428
NS 3	5308	5458	5068	5197	5324
NS 4	5686	5836	5343	5367	5666
NS 5	5649	5799	5353	5338	5633
NS 6	5825	5925	5073	5530	5773
NS 7	5757	5857	5020	5400	5697
NS 8	5618	5718	5393	5457	5613
NS 9	5307	5407	5329	5118	5310
NS 10	5105	5205	4878	5093	5122
NS 11	5136	5136	4903	5075	5115
NS 12	5389	5489	5056	5192	5373
NS 13	5349	5417	5194	5247	5346
NS 14	5168	5268	5042	4919	5154
NS 15	5149	5199	4601	4984	5112

aspect represented as a single curve to understand the response and impact of the glaciers on the landscape. It shows the distribution of the normalize cumulative area with the change in elevation. The hypsometric curve of all glaciers is represented in Fig. 4. The model also provides a spatial estimation of the paleo-ice thickness across the study area, illustrated in Fig. 5. The results indicate an ice thickness approximately ranging between 200 and 400 m, reaching a maximum of about 370 m. This thickest ice was concentrated in the main valley trunk of the largest reconstructed Siachen Glacier (NS1), consistent with ice convergence and accumulation in that part of the valley.

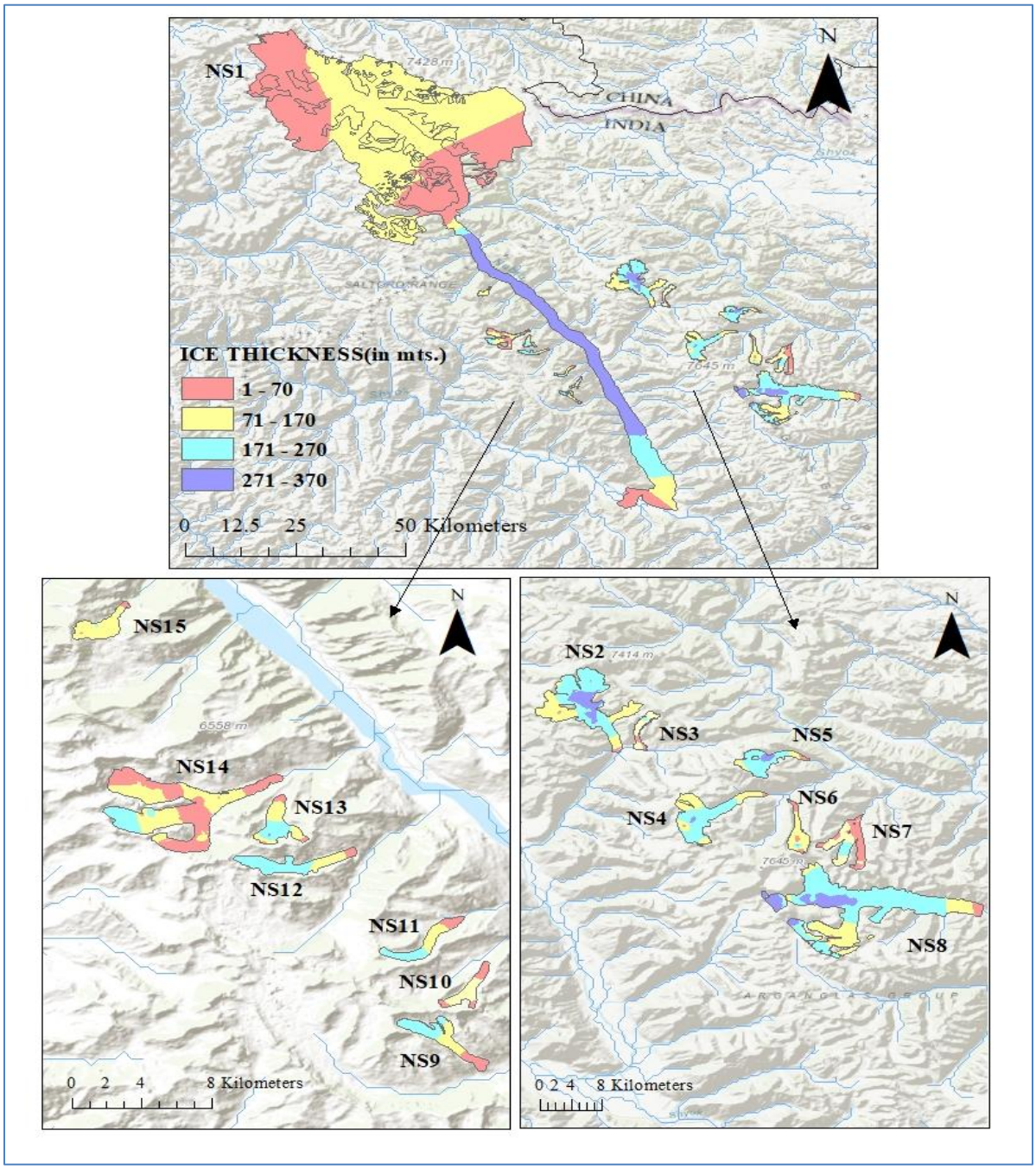

Fig. 5. Map showing the reconstructed ice thickness for the 15 paleo-glaciers (NS1–NS15) in the Nubra-Shyok valley. The spatial distribution of ice thickness (in meters) is shown for the main Siachen trunk glacier (NS1, top panel) and the 14 tributary glaciers (NS2–NS8, bottom-right inset; NS9–NS15, bottom-left inset). The maximum modeled ice thickness (~370 m) is concentrated in the main valley trunk of the Siachen glacier

3.3. *Paleo-Equilibrium Line Altitude (ELA) Estimation*

The ELA values derived from each method (AABR, AAR, MELM, THAR) for all 15 glaciers are presented in Table 1. To assess the consistency between these methods, a correlation matrix was generated (Table 2), which indicates a very strong positive correlation between the AABR and AAR methods (R^2 = 0.992). The final, representative paleo-ELA calculated as WA ELA for each glacier is provided in Table 1 and Fig. 2. The calculated paleo-ELA values for the 15 glaciers range from 4236 m

TABLE 2

Showing the paleo-ELA values estimated by using different ELA methods and then taking weighted average of all the methods to obtain a single value. The weight assigned to each method is mentioned in the table.

	AABR	*AAR*	*MELM*	*THAR*
AABR	1			
AAR	0.992861	1		
MELM	0.818667	0.859295	1	
THAR	0.944293	0.931587	0.819175	1

(NS1) to 5773 m (NS6). The WA-based paleo-ELA values exhibit a moderate degree of variability, with a standard deviation of 377 m around a mean elevation of ~5327 m. The glaciers within the valley display two dominant orientation patterns: a northwest–southeast (NW–SE) trend for the eastern and central glaciers (NS2–NS8) and a northeast–southwest to east–west (NE–SW/E–W) trend for the western glaciers (NS9–NS15). Excluding the Siachen Glacier (NS1), which is an outlier with a markedly low paleo-ELA of 4236 m, the NW–SE-oriented glaciers exhibit paleo-ELA values ranging from 5324 to 5773 m, with a mean of 5590 m, median of 5633 m, and a range of 449 m. In contrast, the NE–SW and E–W-oriented glaciers show more uniform paleo-ELA between 5112 and 5373 m, with a mean of 5219 m, median of 5154 m, and a range of 261 m. The mean ELA difference between the two orientation groups is ~371 m, and the median difference is 479 m, indicating that the NW–SE-oriented glaciers represent significantly higher ELA than the NE–SW-oriented ones. This suggests a clear spatial ELA gradient increasing eastward across the valley.

3.4. *Present-day ELA and ELA Depression*

The present-day ELA for the 15 glaciers was calculated to quantify the total ELA shift since the LGM. The present-day ELA values range from 4947 m (NS1) to 5932 m (NS7), with a mean of 5468 m. The ELA depression, or the difference between the paleo-ELA and the present-day ELA, was then calculated for each glacier. The most significant finding from this comparison is the substantial ELA depression of ~ 711 m calculated for the main Siachen trunk glacier (NS1).

3.5. *Discussion*

The paleo-glacier reconstruction from the Nubra-Shyok valley provides a robust quantitative basis for evaluating Late Quaternary glacier-climate interactions in the Karakoram during the LGM. The pronounced ELA depression of ~700 m estimated for the Siachen trunk glacier (NS1), the principal drainage system in the valley, corresponds to a mean summer temperature reduction of approximately 1.9 °C, assuming an automatic weather stations (AWS)-derived surface lapse rate of 2.73 °C km^{-1}. This lapse rate was calculated from two AWS located on the Siachen Glacier, separated by an elevation difference of 110 m. Although the relatively small vertical separation introduces some uncertainty in the lapse-rate estimation, the derived value is consistent with slope-scale lapse rates (2.5-3.0 °C km^{-1}) reported across Himalayan catchments. Comparable lapse-rate behavior and temperature-altitude relationships have been documented in hydrometeorological studies from the western Himalaya (Thayyen *et al*., 2005; Thayyen & Dimri, 2018), supporting the reliability of the reconstructed paleotemperature estimates. This moderate cooling aligns with regional-scale reconstructions across the interior Karakoram, reflecting a strong influence of the mid-latitude westerlies during the LGM. The intensified westerlies likely enhanced winter precipitation, sustaining expanded glaciers and partially offsetting the full magnitude of global LGM cooling (Tierney *et al*., 2020). The magnitude of this ELA depression thus provides compelling evidence for a major glacial advance during MIS 2, affirming the LGM as a distinct and climatically significant phase in the Nubra–Shyok valley's Quaternary glacial history.

The paleo-ELA of the tributary glaciers exhibit a clear orientation-dependent asymmetry. East-facing (NW–SE-oriented) glaciers record a mean paleo-ELA of 5590 m, whereas west-facing (NE–SW to E–W-oriented) glaciers average 5219 m, indicating a systematic elevation difference of approximately 370 m. This disparity reflects the complex interaction between regional atmospheric circulation and topographic orientation, particularly under the dominance of the westerlies during the LGM. The valley lies deep within the westerly-influenced interior Karakoram, receiving most of its winter and spring precipitation from these atmospheric circulations (Ganju *et al*., 2018; Palazzi *et al*., 2013). During the LGM, paleoclimatic reconstructions indicate that the westerlies intensified and migrated equatorward (Juyal *et al*., 2014; Owen & Dortch, 2014), enhancing orographic snowfall on windward slopes while expanding the precipitation shadow on leeward slopes. Consequently, west-facing glaciers, exposed directly to these moisture-bearing winds, maintained mass balance at lower, warmer altitudes, whereas east-facing glaciers, situated in the leeward rain shadow of the valley, required higher ELA to sustain equilibrium. In addition, differences in solar radiation likely strengthened this contrast. East- facing slopes most likely receives more morning sunlight and experience greater melt, whereas west-facing slopes, often obscured by afternoon cloud buildup from westerly systems,

undergo reduced ablation (Ganju *et al*., 2018). The combined influence of moisture availability and insolation asymmetry thus emerges as the dominant local control on glacier equilibrium during the LGM, reaffirming the westerly-dominated paleoclimate regime of the interior Karakoram.

The reconstructed modelled ice thickness of ~370 m for the Siachen trunk glacier implies a high-capacity erosional process capable of major valley modification. This is consistent with field observations of classic U-shaped troughs, polished bedrock, and striated surfaces, indicating substantial over deepening during the LGM (Juyal *et al*., 2014). The magnitude of ice cover would have generated significant volumes of glaciofluvial sediment, contributing to the valley-fill deposits and alluvial fans that dominate the lower reaches of the Nubra–Shyok valley. Importantly, this glacier operated within a tectonically active landscape, controlled by the Karakoram Fault (Hakhoo *et al*., 2019). The active tectonism sustains the extreme relief necessary for glacier formation while simultaneously influencing valley orientation and drainage pathways. The structural lineaments impose first-order controls on valley direction, thereby modulating exposure to moisture-bearing winds and ultimately influencing glacier mass balance (Hakhoo *et al*., 2019). The preservation of moraines from multiple Pleistocene advances indicates that, despite ongoing uplift, certain intervals of relative tectonic stability permitted the accumulation and survival of these geomorphic archives. These interactions between tectonic uplift, topographic control, and glacial processes are crucial to understanding the complex landscape evolution of the valley.

The LGM glaciation in the valley aligns closely with well-established regional chronologies, indicating a major glacial advance during MIS-2 (~18–24 ka), contemporaneous with the Deshkit-I/Tirith-I moraines (Ganju *et al*., 2018; Sharma *et al*., 2018; Bhardwaj *et al*., 2024). The OSL ages from the Agham, Khardung, Changmar, and Chalunka sections reported by Bhardwaj *et al*. (2024) further substantiate this phase, documenting extensive glacier and down-valley expansion during the LGM, consistent with enhanced winter precipitation from intensified westerlies. These findings correlate with comparable ages from the upper Shyok and Khardung valleys (~24 ± 2.4 ka to ~18 ± 2.0 ka), reflecting a synchronous valley-wide glacial advance. The subsequent retreat phases identified at ~14.5–13.0 ka, ~8.2–6.0 ka, and ~2.4–0.4 ka correspond to late glacial, early-to-mid Holocene, and Neoglacial intervals respectively (Bhardwaj *et al*., 2024; Ganju *et al*., 2018), each marking climatically driven glacier readvances linked to short-term cooling events such as the Younger Dryas and the Little Ice Age. The older moraine, Deshkit-II/Tirith-II (~60–80 ka; MIS-4) and Deshkit-III (~145 ka; MIS-6), reported by Dortch *et al*. (2010) further indicate repeated late Quaternary glacial oscillations under the influence of westerlies. Collectively, these chronologies affirm the valley's sensitivity to global climatic oscillations modulated by regional moisture availability, with the strongest glacial imprint formed under enhanced westerlies during the LGM. However, the lack of direct numerical dating of the moraine ridges used for ELA reconstruction limits chronological precision and highlights the need for future geochronological constraints to better link reconstructed glacier extents with global climate phases.

4. Conclusions

The present study reconstructed the geometry of LGM paleo-glaciers and their corresponding ELAs for 15 glaciers in the Nubra-Shyok valley. The results provide new quantitative insights into the paleoclimatic and geomorphic conditions of this westerly-dominated region.

(i) The Siachen trunk glacier (NS1), the principal drainage system of the valley, experienced a mean ELA depression of approximately 700 m relative to present. Using the regional lapse rate (2.3 °C/km), this depression corresponds to a summer temperature cooling of about 1.5–2.0 °C. This moderate yet significant cooling confirms the occurrence of a major glacial advance during the global LGM (MIS-2), consistent with enhanced moisture delivery from intensified westerlies.

(ii) The paleo-ELA distribution reveals a pronounced aspect-related asymmetry, with west-facing glaciers exhibiting significantly lower mean ELAs (5246 m) than east-facing glaciers (5590 m). This pattern reflects the combined influence of enhanced orographic precipitation on windward slopes and reduced ablation due to lower insolation and increased afternoon cloud cover demonstrating that glacier mass balance in the valley during the LGM was strongly governed by westerly-derived moisture and local topographic factors.

Overall, these findings highlight a major LGM glacial episode in the Nubra–Shyok valley, driven by the interplay between regional atmospheric circulation and global cooling. The reconstructed glacial geometries and ELAs provide an important benchmark for understanding Quaternary climate variability in the interior Karakoram. However, as the chronological framework relies on morpho stratigraphic correlation rather than absolute dating, the temporal attribution of the reconstructed glacial stage remains provisional. Future chronological investigations particularly using cosmogenic nuclide

(^{10}Be) or OSL dating are essential to precisely constrain the timing of the reconstructed advances and refine the Quaternary glacial history.

Data availability

The authors confirm that the data supporting the findings of this study are available within the article.

Acknowledgments

The authors are thankful to the Director of DGRE, DRDO for providing the necessary computational help to conduct the research work in the lab. We are thankful to the Director, CSIO-CSIR to allow us to carry out the present study. We are grateful for the constructive comments by the reviewers which helped us in enhancing quality of the manuscript.

Authors' contributions

Pranshu Bhardwaj: Conceptualization; Data curation; Formal analysis; Writing-original draft; and Writing - review & editing.
Y.C.Nagar: Conceptualization, Methodology; Supervision; Validation; Writing - review & editing.
Tejpal Singh: Supervision; Validation; Writing- review & editing.(*email- yc.nagar.dgre@gov.in*).
M.S.Shekhar: Supervision; Validation; Writing - review & editing.(*email- sudhanshu.dgre@gov.in*)

Disclaimer: The contents and views presented in this research article/paper are the views of the authors and do not necessarily reflect the views of the organizations they belong to.

References

Benn, D.I. and Lehmkuhl, F., 2000, "Mass balance and equilibrium-line altitudes of glaciers in high-mountain environments", *Quaternary International*, 65, 15–29. https://doi.org/10.1016/S1040-6182(99)00034-8.

Benn, D.I. and Owen, L.A., 1998, "The role of the Indian summer monsoon and the mid-latitude westerlies in Himalayan glaciation: review and speculative discussion", Journal of the Geological Society, 155(2), 353–363. https://doi.org/10.1144/gsjgs.155.2.0353.

Bhardwaj, P., Nagar, Y.C., Singh, T., Shekhar, M.S. and Ganju, A., 2024, "Reconstruction of landscape change of Shyok Valley, Ladakh during Late Quaternary using OSL technique", Quaternary International, 710, 1-17. https://doi.org/10.1016/j.quaint.2024.08.010.

Bhutiyani, M.R., Kale, V.S. and Pawar, N.J., 2010, "Climate change and the precipitation variations in the northwestern Himalaya: 1866–2006", International Journal of Climatology, 30(4), 535. https://doi.org/10.1002/joc.1920.

Bolch, T., Kulkarni, A., Kääb, A., Huggel, C., Paul, F., Cogley, J.G., Frey, H., Kargel, J.S., Fujita, K., Scheel, M. and Bajracharya, S., 2012, "The state and fate of Himalayan glaciers", Science, 336(6079), 310–314. DOI: 10.1126/science.1215828

Chevuturi, A., Dimri, A.P. and Thayyen, R.J., 2018, "Climate change over Leh (Ladakh), India", Theoretical and Applied Climatology, 131(1), 531–545. DOI: 10.1007/s00704-016-1989-1

Cogley, J.G., Arendt, A.A., Bauder, A., Braithwaite, R.J., Hock, R., Jansson, P., Kaser, G., Moller, M., Nicholson, L., Rasmussen, L.A. and Zemp, M., 2010, "Glossary of glacier mass balance and related terms". DOI: 10.5167/uzh-53475

Damm, B., 2006, "Late Quaternary glacier advances in the upper catchment area of the Indus River (Ladakh and western Tibet)", Quaternary International, 154, 87–99. DOI:10.1016/J.QUAINT.2006.02.013

Dash, S.K., Singh, G.P., Vernekar, A.D. and Shekhar, M.S., 2004, "A study on the number of snow days over Eurasia, Indian rainfall and seasonal circulations", Meteorology and Atmospheric Physics, 86(1), 1–13. https://doi.org/10.1007/s00703-003-0016-0

Dortch, J.M., Owen, L.A. and Caffee, M.W., 2010, "Quaternary glaciation in the Nubra and Shyok Valley confluence, northernmost Ladakh, India", Quaternary Research, 74(1), 132–144. http://dx.doi.org/10.1016/j.yqres.2010.04.013

Ganju, A., Nagar, Y.C., Sharma, L.N., Sharma, S. and Juyal, N., 2018, "Luminescence chronology and climatic implication of the Late Quaternary glaciation in the Nubra Valley, Karakoram Himalaya, India", Palaeogeography, Palaeoclimatology, Palaeoecology, 502, 52–62. https://doi.org/10.1016/j.palaeo.2018.04.022

GLIMS, N., 2018, "Global land ice measurements from space glacier database". Compiled and made available by the international GLIMS community and the National Snow and Ice Data Center, Boulder CO, USA. https://doi. org/10.7265/N5V98602

Greenwood, S.L. and Clark, C.D., 2009, "Reconstructing the last Irish Ice Sheet 2: a geomorphologically-driven model of ice sheet growth, retreat and dynamics", Quaternary Science Reviews, 28(27–28), 3101–3123. https://doi.org/10.1016/j.quascirev.2009.09.014

Haeberli, W., Gärtner-Roer, I., Hoelzle, M., Paul, F. and Zemp, M., 2009, "WGMS 2009: Glacier Mass Balance Bulletin No. 10 (2006–2007)", Glacier Mass Balance Bulletin, 10.

Hakhoo, N., Bhat, G.M., Pandita, S., Hussain, G., Haq, A.U., Hafiz, M., Ahmed, W., Singh, Y. and Thusu, B., 2019, "Natural hazards—their drivers, mechanisms and impacts in the Shyok–Nubra Valley, NW Himalaya, India", International Journal of Disaster Risk Reduction, 35, 101094. DOI: 10.1016/j.ijdrr.2019.101094

Herzschuh, U., 2006, "Palaeo-moisture evolution in monsoonal Central Asia during the last 50,000 years", Quaternary Science Reviews, 25(1–2), 163–178. https://doi.org/10.1016/j.quascirev.2005.02.006.

Hewitt, K., 2005, "The Karakoram anomaly? Glacier expansion and the 'elevation effect', Karakoram Himalaya", Mountain Research and Development, 25, 332–340. http://dx.doi.org/10.1659/0276-4741(2005)025[0332:TKAGEA]2.0.CO;2.

Immerzeel, W.W., Van Beek, L.P. and Bierkens, M.F., 2010, "Climate change will affect the Asian water towers", Science, 328(5984), 1382–1385. DOI: 10.1126/science.1183188.

Jansson, K.N. and Glasser, N.F., 2005, "Using Landsat 7 ETM+ imagery and digital terrain models for mapping glacial lineaments on former ice sheet beds", International Journal of Remote Sensing, 26(18), 3931–3941. DOI:10.1080/01431160500106900.

Juyal, N., 2014, "Ladakh: the high-altitude Indian cold desert", in Landscapes and Landforms of India, Dordrecht: Springer Netherlands, 115–124. DOI:10.1007/978-94-017-8029-2_10.

Kurowski, L., 1891, "Die Höhe der Schneegrenze mit besonderer Berücksichtigung der Finsteraarhorn-Gruppe", Selbstverlag.

Murari, M.K., Owen, L.A., Dortch, J.M., Caffee, M.W., Dietsch, C., Fuchs, M., Haneberg, W.C., Sharma, M.C. and Townsend-Small, A., 2014, "Timing and climatic drivers for glaciation across monsoon-influenced regions of the Himalayan–Tibetan orogen", Quaternary Science Reviews, 88, 159–182. https://doi.org/10.1016/j.quascirev.2014.01.013.

Nagar, Y.C., Ganju, A., Satyawali, P.K. and Juyal, N., 2013, "Preliminary optical chronology suggests significant advance in Nubra Valley glaciers during the Last Glacial Maximum", Current Science, 105, 96–101.

Nye, J.F., 1952a, "A method of calculating the thicknesses of the ice-sheets", Nature, 169, 529–530. DOI:10.1038/169529a0.

Nye, J.F., 1952b, "The mechanics of glacier flow", Journal of Glaciology, 2, 82–93. DOI: 10.3189/S0022143000033967

Oerlemans, J., 2005, "Extracting a climate signal from 169 glacier records", Science, 308(5722), 675–677. DOI: 10.1126/science.1107046.

Osmaston, H., 2005, "Estimates of glacier equilibrium line altitudes by the Area × Altitude, the Area × Altitude Balance Ratio and the Area × Altitude Balance Index methods and their validation", Quaternary International, 138, 22–31. DOI: 10.1016/j.quaint.2005.02.004.

Owen, L.A. and Benn, D.I., 2005, "Equilibrium-line altitudes of the Last Glacial Maximum for the Himalaya and Tibet: an assessment and evaluation of results", Quaternary International, 138, 55–78. https://doi.org/10.1016/j.quaint.2005.02.006.

Owen, L.A. and Dortch, J.M., 2014, "Nature and timing of Quaternary glaciation in the Himalayan–Tibetan orogen", Quaternary Science Reviews, 88, 14–54. http://dx.doi.org/10.1016/j.quascirev.2013.11.016.

Palazzi, E., Von Hardenberg, J. and Provenzale, A., 2013, "Precipitation in the Hindu Kush Karakoram Himalaya: observations and future scenarios", Journal of Geophysical Research: Atmospheres, 118(1), 85–100. https://doi.org/10.1029/2012JD018697.

Paul, O.J., Dar, R.A. and Romshoo, S.A., 2022, "Paleo-glacial and paleo-equilibrium line altitude reconstruction from the Late Quaternary glacier features in the Pir Panjal Range, NW Himalayas", Quaternary International, 642, 5–16. DOI:10.1016/j.quaint.2021.03.005.

Pellitero, R., Rea, B.R., Spagnolo, M., Bakke, J., Hughes, P., Ivy-Ochs, S., Lukas, S. and Ribolini, A., 2015, "A GIS tool for automatic calculation of glacier equilibrium-line altitudes", Computers & Geosciences, 82, 55–62. DOI:10.1016/j.cageo.2015.05.005.

Pellitero, R., Rea, B.R., Spagnolo, M., Bakke, J., Ivy-Ochs, S., Frew, C.R., Hughes, P., Ribolini, A., Lukas, S. and Renssen, H., 2016, "GlaRe, a GIS tool to reconstruct the 3D surface of palaeoglaciers", Computers & Geosciences, 94, 77–85. https://doi.org/10.1016/j.cageo.2016.06.008.

Porter, S.C., 2000, "Snowline depression in the tropics during the Last Glaciation", Quaternary Science Reviews, 20(10), 1067–1091. https://doi.org/10.1016/S0277-3791(00)00178-5.

Raina, V.K. and Sangewar, C., 2007, "Siachen Glacier of Karakoram Mountains, Ladakh—its secular retreat", Geological Society of India, 11–16. https://doi.org/10.17491/jgsi/2007/700102.

Rea, B.R., 2009, "Defining modern day Area–Altitude Balance Ratios (AABRs) and their use in glacier–climate reconstructions", Quaternary Science Reviews, 28(3–4), 237–248. https://doi.org/10.1016/j.quascirev.2008.10.011.

Searle, M.P., Weinberg, R.F. and Dunlap, W.J., 1998, "Transpressional tectonics along the Karakoram fault zone, northern Ladakh: constraints on Tibetan extrusion", Geological Society, London, Special Publications, 135(1), 307–326. DOI:10.1144/GSL.SP.1998.135.01.20.

Sharma, S., Hussain, A., Mishra, A.K., Lone, A., Solanki, T. and Khan, M.K., 2018, "Geomorphic investigation of the Late-Quaternary landforms in the southern Zanskar Valley, NW Himalaya", Journal of Earth System Science, 127(1), 9. DOI: 10.1007/s12040-017-0911-2.

Shekhar, M.S., Devi, U., Paul, S., Singh, G.P. and Singh, A., 2017, "Analysis of trends in extreme precipitation events over Western Himalaya region: intensity- and duration-wise study", Journal of Indian Geophysical Union, 21(3), 223–229.

Thakur, V.C. and Misra, D.K., 1984, "Tectonic framework of the Indus and Shyok suture zones in eastern Ladakh, northwest Himalaya", Tectonophysics, 101(3–4), 207–220. https://doi.org/10.1016/0040-1951(84)90114-8.

Thayyen, R.J. and Dimri, A.P., 2018, "Slope environmental lapse rate (SELR) of temperature in the monsoon regime of the western Himalaya", Frontiers in Environmental Science, 6, 42. https://doi.org/10.3389/fenvs.2018.00042.

Thayyen, R.J., Gergan, J.T. and Dobhal, D.P., 2005, "Lapse rate of slope air temperature in a Himalayan catchment—a study from Din Gad (Dokriani Glacier) basin, Garhwal Himalaya, India", Bulletin of Glaciological Research, 22, 19–25.

Tierney, J.E., Zhu, J., King, J., Malevich, S.B., Hakim, G.J. and Poulsen, C.J., 2020, "Glacial cooling and climate sensitivity revisited", Nature, 584(7822), 569–573. DOI: 10.1038/s41586-020-2617-x

Upadhyay, R., Sinha, A.K., Chandra, R. and Rai, H., 1999, "Tectonic and magmatic evolution of the eastern Karakoram, India", Geodinamica Acta, 12(6), 341–358. DOI:10.1080/09853111.1999.11105354.

Weinberg, R.F. and Searle, M.P., 1998, "The Pangong Injection Complex, Indian Karakoram: a case of pervasive granite flow-through hot viscous crust", Journal of the Geological Society, 155(5), 883–891. https://doi.org/10.1144/gsjgs.155.5.0883.